Electronic Supplementary Material (ESI) for Journal of Materials Chemistry C.

Slow magnetic relaxation and luminescence properties in β-diketonate lanthanide(III) complexes. Preparation of Eu(III) and Yb(III) OLED devices.

Ànnia Tubau, Laura Rodríguez, Piotr Pander, Lucy Weatherill, Fernando B. Dias, Mercè Font-Bardía, Ramon Vicente.

Elemental analysis and Infrared Spectroscopy.

Compilation of the bands seen in the infrared spectra of compounds **1-Sm** to **6-Yb**.

[Sm(Btfa)$_3$(4,4'-dinonyl-2,2'-bipy)] (**1-Sm**): Anal. Calc. For $C_{58}H_{62}SmF_9N_2O_6$ (1108.4 g/mol): C, 62.8; N, 2.5; H, 5.6 %. Found: C, 62.4; N, 2.5; H, 5.6 %. Selected IR bands (ATR-IR, cm^{-1}): 2928.6(m), 2858.5(m), 1608.5(s), 1573.4(m, split), 1522.4(m, split), 1318.3(m), 1292.8(s), 1241.8(m), 1184.4(s), 1133.4(s), 1076.0(m), 1015.4(m), 945.3(m), 763.5(s), 702.9(s), 632(m), 578.57(m). (Fig. S2)

[Eu(Btfa)$_3$(4,4'-dinonyl-2,2'-bipy)] (**2-Eu**): Anal. Calc. For $C_{58}H_{62}EuF_9N_2O_6$ (1110.0 g/mol): C, 62.8; N, 2.5; H, 5.6 %. Found: C, 62.1; N, 2.4; H, 5.8 %. Selected IR bands (ATR-IR, cm^{-1}): 2924.0(m), 2847.6(m), 1612.2.5(s), 1569,0(m, split), 1525.8(m, split), 1472.7(m), 1293.4(s), 1246.9(l), 1183.8(s), 1133.4(s), 1120.7(s), 1015.4(m), 1070.9(l), 781.9(s), 679.0(s), 562.7(m).

[Tb(Btfa)$_3$(4,4'-dinonyl-2,2'-bipy)] (**3-Tb**): Anal. Calc. For $C_{58}H_{62}TbF_9N_2O_6$ (1117.0g/mol): C, 62.4; N, 2.5; H, 5.6 %. Found: C, 62.2; N, 2.4; H, 5.6 %. Selected IR bands (ATR-IR, cm^{-1}): 2924.0(m), 2854.2(m), 1605.5(s), 1572.3(m), 1519.2(m), 1476.0(m), 1286.7(s), 1183.8(s), 1124.0(s), 1074.2(m), 1076.0(m), 762.0(m), 945.3(m), 692.3(m), 702.9(s), 625.8(m), 576.0(m).

[Dy(Btfa)$_3$(4,4'-dinonyl-2,2'-bipy)] (**4-Dy**): Anal. Calc. For $C_{58}H_{62}DyF_9N_2O_6$ (1120.6 g/mol): C, 62.2; N, 2.5; H, 5.6 %. Found: C, 62.2; N, 2.3; H, 5.5 %. Selected IR bands (ATR-IR, cm^{-1}): 2924.0(m), 2850.9(m), 1608.9(s), 1572.3(m), 1522.5(m, split), 1483.0(m, split), 1293.4(s), 1236.9(m), 1183.7(s), 1133.9(s), 1067.5(m), 1014.4(m), 945.3(m), 938.0(m), 758.7(s), 695.6(m), 629.2(m), 576.0(m).

[Er(Btfa)$_3$(4,4'-dinonyl-2,2'-bipy)] (**5-Er**): Anal. Calc. For $C_{58}H_{62}ErF_9N_2O_6$ (1125.3 g/mol): C, 61.9; N, 2.5; H, 5.6 %. Found: C, 61.8; N, 2.7; H, 5.6 %. Selected IR bands (ATR-IR, cm^{-1}): 2920.6(m), 2854.2(m), 1605.5(s), 1572.3(m), 1522.5(m, split), 1479.3(m, split), 1290.0(s), 1240.2(m), 1183.8(s), 1127.3(s), 1067.5(m), 1007.7(l), 762.0(m), 695.6(m), 625.8(m), 695.6(m), 576.0(m).

[Yb(Btfa)$_3$(4,4'-dinonyl-2,2'-bipy)] (**6-Yb**): Anal. Calc. For $C_{58}H_{62}YbF_9N_2O_6$ (1131.1 g/mol): C, 61.6; N, 2.5; H, 5.5 %. Found: C, 61.7; N, 2.7; H, 5.3 %. Selected IR bands (ATR-IR, cm^{-1}): 2927.3(m), 2850.9(m), 1605.5(s), 1569.0(m), 1519.2(m, split), 1486.0(m, split), 1290.0(s), 1240.2(m), 1177.1(s), 1127.3(s), 1070.9(m), 1011.1(l), 944.7(l), 758.7(s), 695.6(s), 625.8(m), 576.0(m).

[Gd(Btfa)$_3$(4,4'-dinonyl-2,2'-bipy)] (**7-Gd**): Selected IR bands (ATR-IR, cm^{-1}): 2927.3(m), 2850.9(m), 1605.5(s), 1575.6(m), 1522.5(m, split), 1479.3(m, split), 1286.7(s), 1236.9(m), 1177.1(s), 1184.7(s), 1130.6(s), 1074.2(l), 1011.0(l), 941.3(s), 758.6(s), 698.9(s), 625.8(m), 579.3(m), 509.6(l), 463.1(l).

1.1 **Structure determination:**

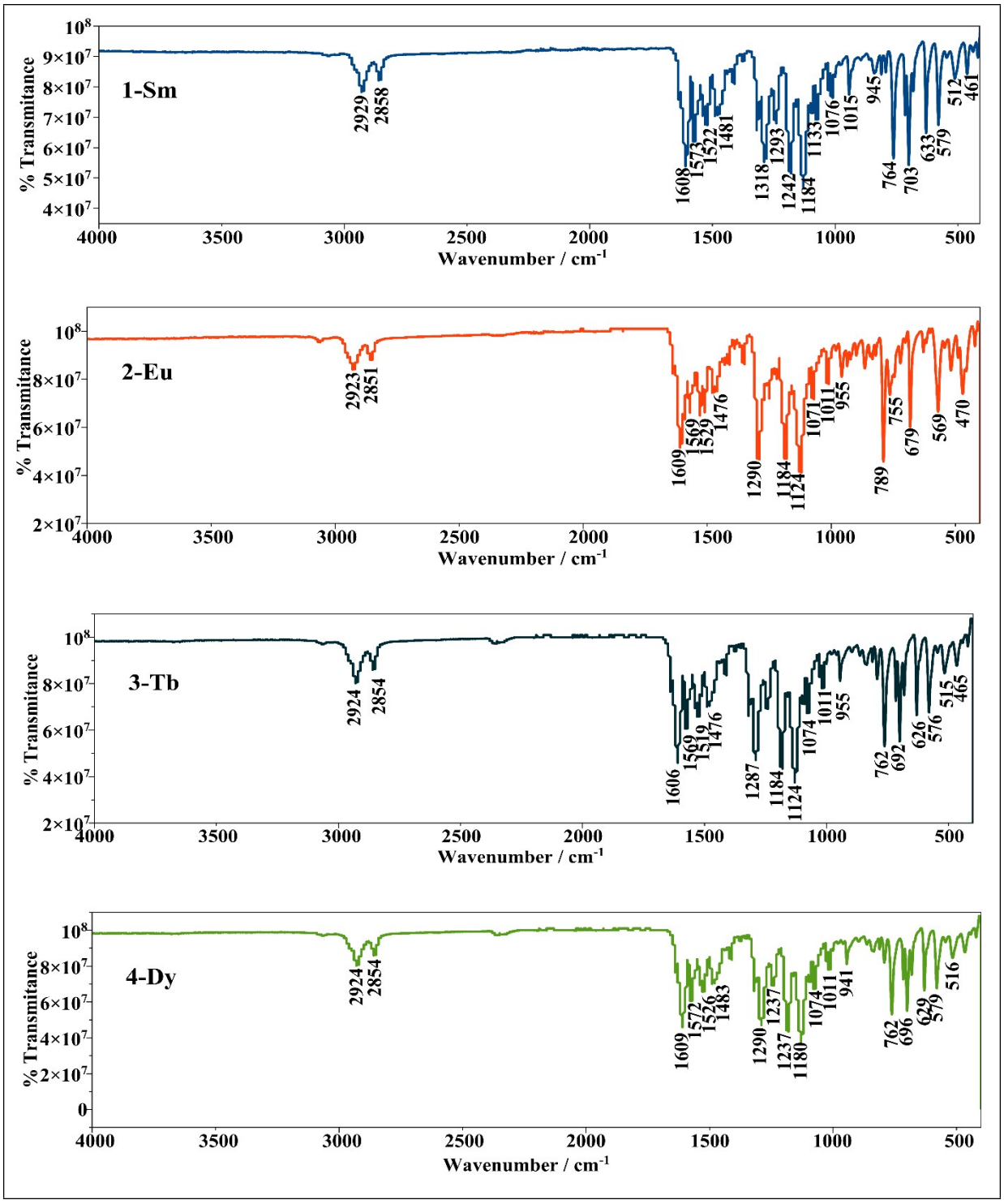
1-Sm
% Transmitance
Wavenumber / cm-1
2929
2858
1608
1573
1522
1481
1318
1293
1242
1184
1133
1076
1015
945
764
703
633
579
512
461
2-Eu
2923
2851
1609
1569
1520
1476
1290
1184
1124
1071
1011
955
789
755
679
569
470
3-Tb
2924
2854
1606
1569
1519
1476
1287
1184
1124
1074
1011
955
762
692
626
576
515
465
4-Dy
2924
2854
1609
1572
1526
1483
1290
1237
1237
1180
1074
1011
941
762
696
629
579
516

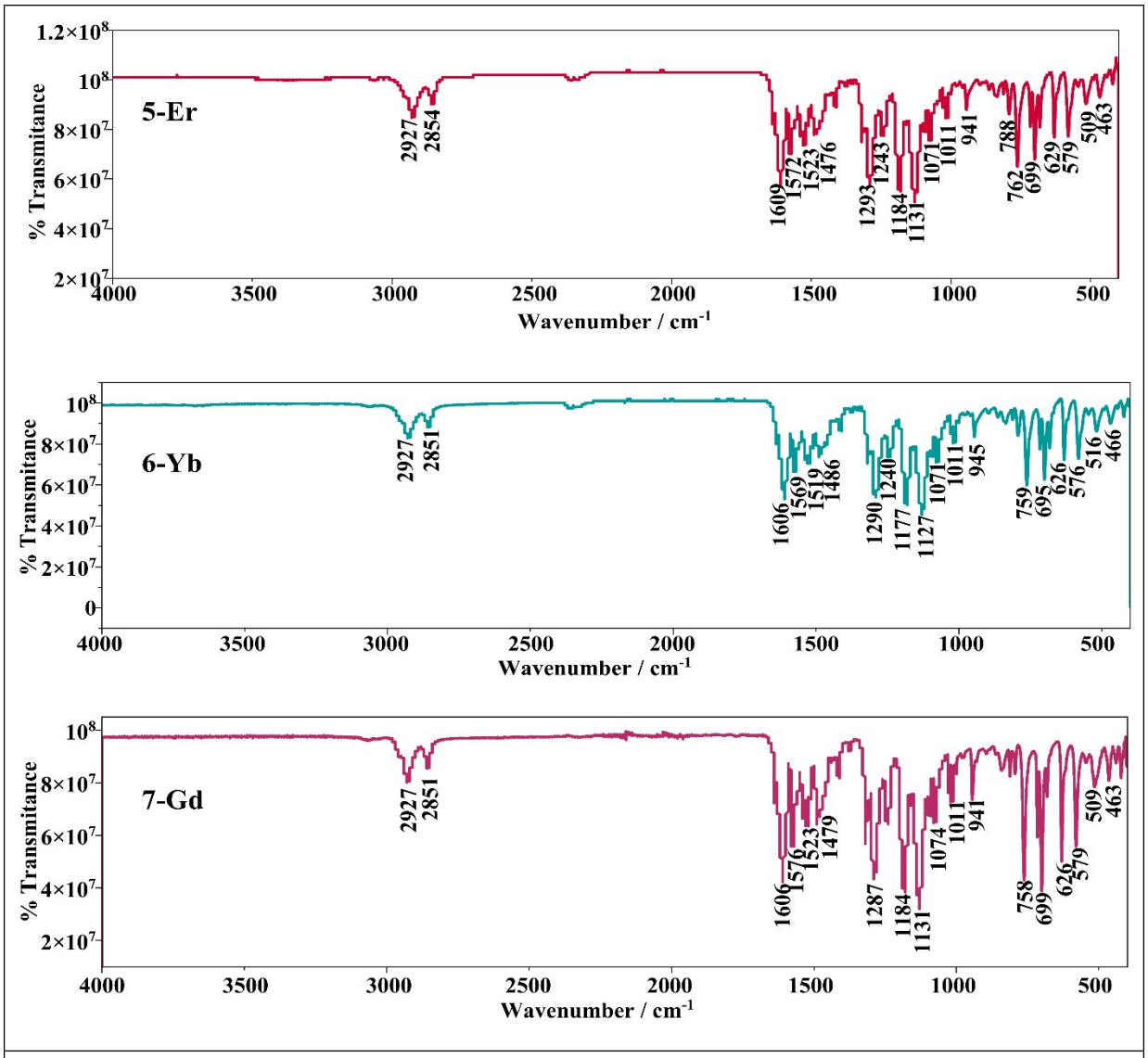

Fig. S1. Infrared spectra of compounds **1-Sm** to **7-Gd**.

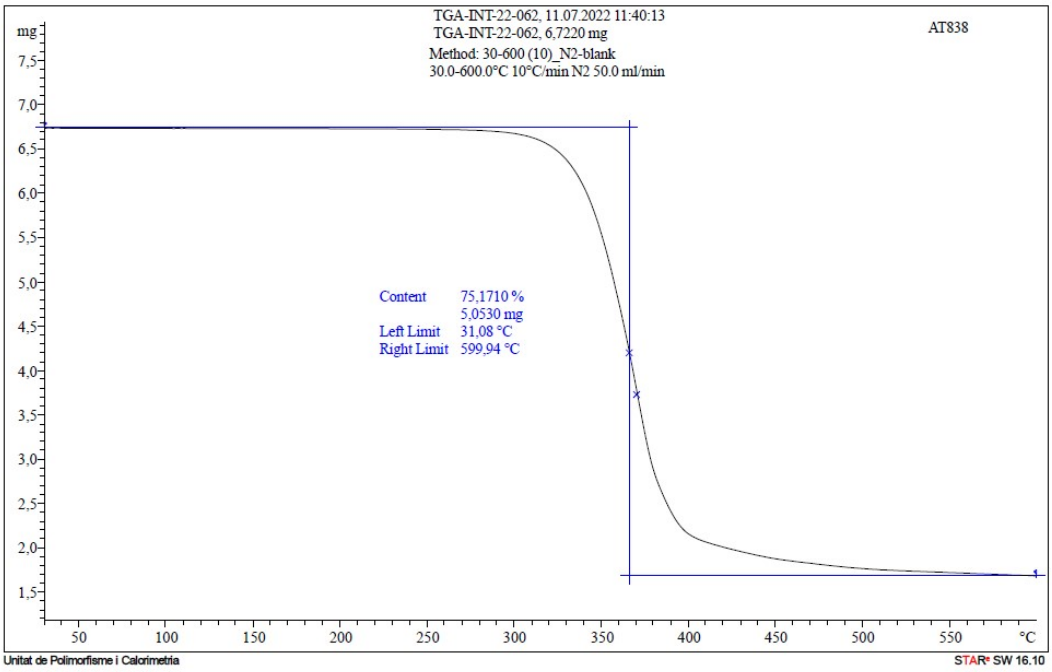

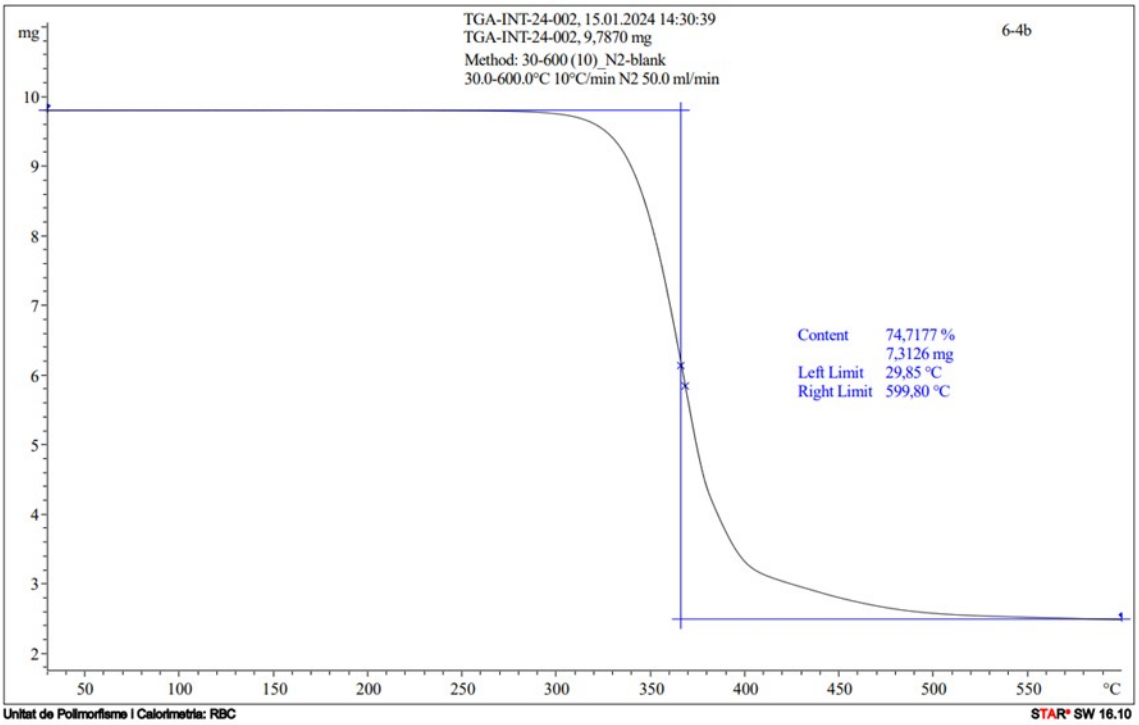

Fig. S2. Thermogravimetric curve of compounds **2-Eu** (top) and **6-Yb** (bottom).

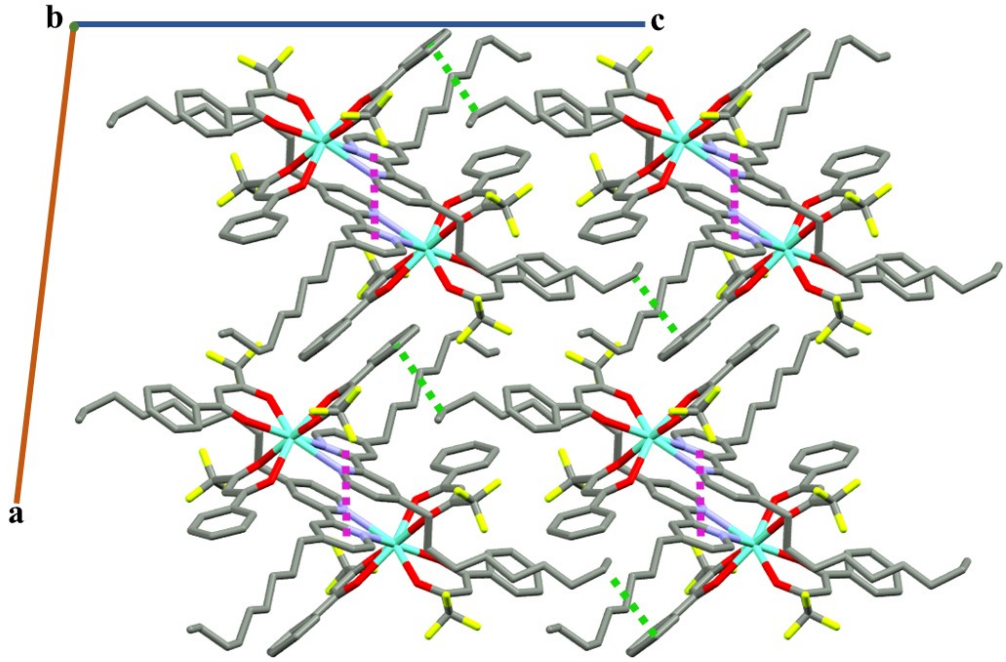

Fig. S3 Crystal packing of compound **2-Eu.** No intermolecular interactions are considered. The shortest Cg-Cg distance is 3.938 Å from the pyridine ring constituted by N1, C31, C32, C33 C34, C35 atoms. The shortest H-pi interaction is 2.7 Å from the ring of one β-diketone molecule and one hydrogen from the alkyl chain. All in all, the distances of the intermolecular interactions are large enough to consider isolated mononuclear systems packed in the crystal lattice.

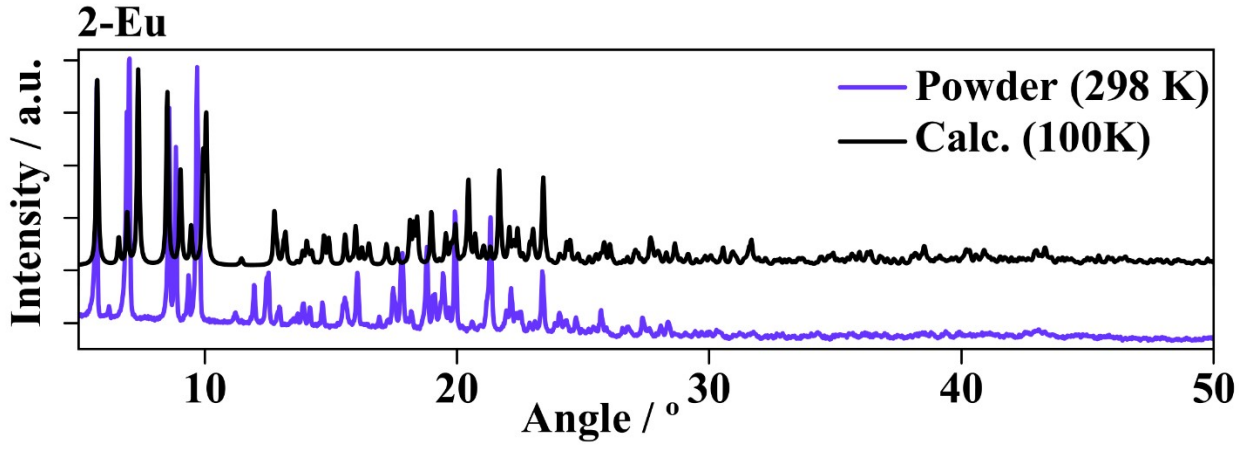

Fig. S4 Powder X-Ray Diffraction pattern of the powder of sample **2-Eu** compared to the Pattern calculated from the Single Crystal structure. Powder X-Ray Diffraction is measured at room temperature (298 K) and the Single crystal structure is measured at 77 K.

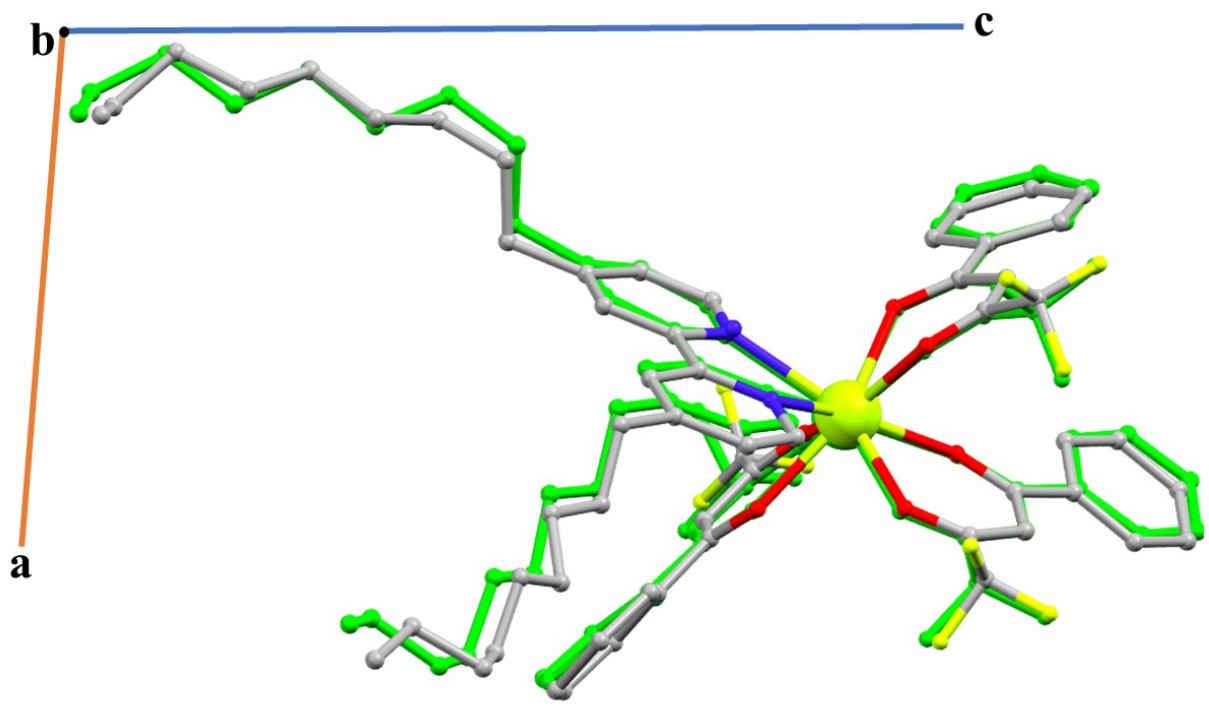

Fig.S5. Single crystal structure overlay of compound **1-Eu** measured at 77K (green) and compound **3-Tb** measured at 304 K (default colours).

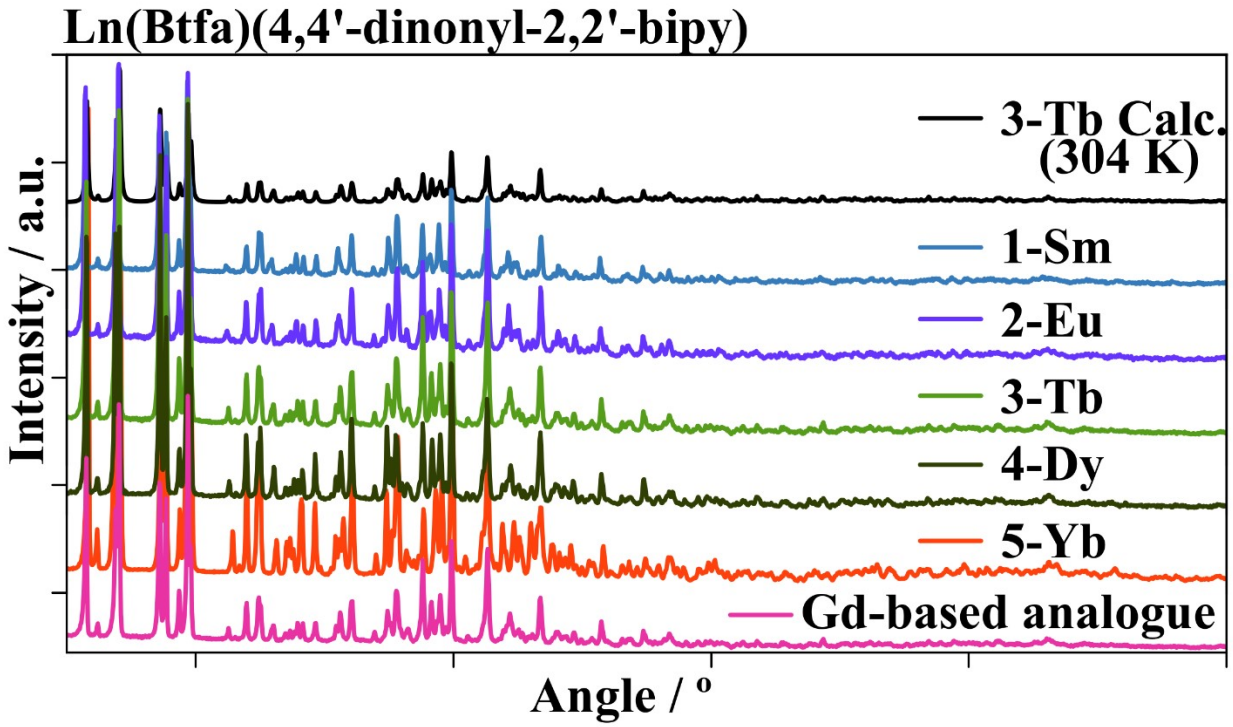

Fig. S6. Powder X-Ray Diffraction pattern of samples **1-Sm** to **5-Yb** and the Gadolinium isostructural analogue measured at room temperature (298K) compared to the pattern calculated from the Single Crystal structure measured at 304 K.

Table S1. Crystallographic information from the Single Crystal X-Ray Diffraction measurements of compounds **2-Eu**, **4-Dy** and **5-Yb**

Complex	**2-Eu**	**4-Dy**	**6-Yb**	**3-Tb**
Formula	$C_{58}H_{62}EuF_9N_2O_6$	$C_{58}H_{62}DyF_9N_2O_6$	$C_{58}H_{62}F_9N_2O_6Yb$	$C_{58}H_{62}F_9N_2O_6Tb$
FW [g/mol]	1206.05	1216.59	1227.14	1213.01
Crystal System	triclinic	triclinic	triclinic	Triclinic
Space Group	P-1	P-1	P-1	P-1
a [Å]	12.8601(5)	12.8613(12)	12.8760(8)	12.8570(6)
b [Å]	14.0622(7)	14.1376(14)	14.2205(9)	14.9805(7)
c [Å]	16.1521(7)	16.0565(15)	15.9478(10)	16.1248(8)
α[º]	106.558(2)	106.879(4)	107.041(2)	107.762(2)
β [º]	94.495(2)	94.113(4)	93.862(2)	93.451(2)
γ [º]	94.606(2)	94.906(4)	94.880(2)	93.871(2)
V [Å^3]	2775.1(2)	2769.2(5)	2768.7(3)	2940.2(2)
Z	2	2	2	2
T[K]	100	100	100	304(2)
λ(Mo kα) [Å]	0.71073	0.71073	0.71073	0.71073
D_{calc} [g cm^{-3}]	1.443	1.459	1.472	1.370
μ(Mo Kα) [mm^{-1}]	1.211	1.430	1.770	1.279
R	0.0410	0.0421	0.0373	0.0761
wR_2	0.0817	0.1076	0.0863	0.2564

Table S2. Selected bond distances (Å) for **2-Eu, 4-Dy and 6-Yb.**

	2-Eu	**4-Dy**	**6-Yb**
Ln-O1	2.389(2)	2.333(3)	2.283(2)
Ln-O2	2.362(2)	2.311(3)	2.268(19)
Ln-O3	2.343(2)	2.320(3)	2.292(2)
Ln-O4	2.351(2)	2.311(3)	2.270(18)
Ln-O5	2.364(2)	2.320(3)	2.278(2)
Ln-O6	2.353(2)	2.355(3)	2.315(19)
Ln-N1	2.559(3)	2.527(3)	2.488(2)
Ln-N2	2.575(3)	2.540(3)	2.489(2)
Shortest Ln---Ln	8.9668	8.921	8.920

1.1 Luminescence measurements:

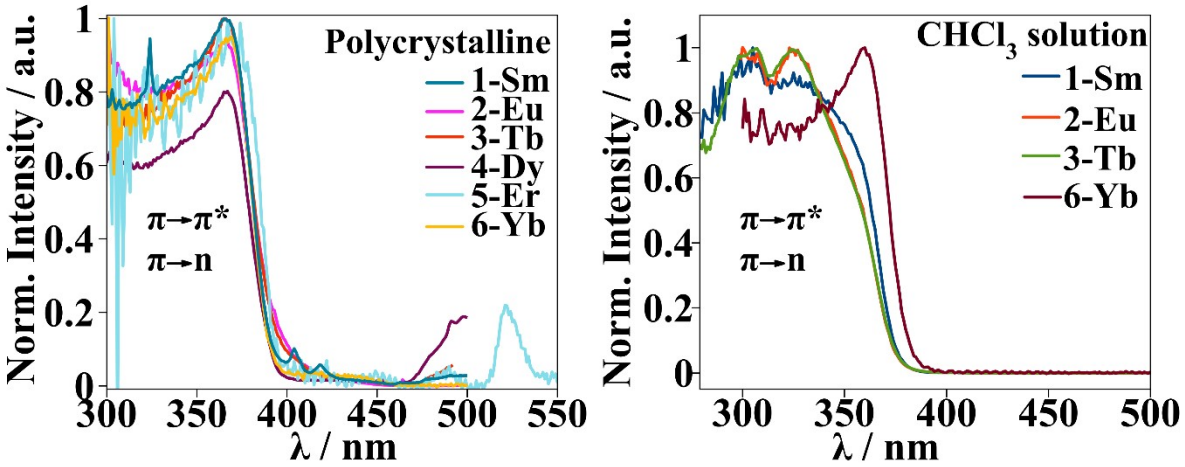

Figure S7. Excitation spectra of the polycrystalline samples (left) and $CHCl_3$ solutions (right) of compounds **1-Sm** to **6-Yb** measured at the emission wavelength (λ_{em}) of 650 nm ($^4G_{5/2}\rightarrow{}^6H_{9/2}$) for **1-Sm**, at 614 nm ($^5D_0\rightarrow{}^7F_2$) for **2-Eu**, at 546 nm ($^5D_4\rightarrow{}^7F_5$) for **3-Tb**, at 577 nm ($^4F_{9/2}\rightarrow{}^6H_{13/2}$) for **4-Dy**, at 1526 nm ($^4I_{13/2}\rightarrow{}^4I_{15/2}$) for **5-Er** and at 1027 nm ($^5F_{5/2}\rightarrow{}^2F_{7/2}$) for **6-Yb**. The peak appearing at 325 nm in the solid state excitation spectra of compound **1-Sm** corresponds to an harmonic signal of the lamp replica. Reliably excitation spectra could not be obtained for the 10^{-6} M chloroform solutions containing compounds **4-Dy** and **5-Er** because of the poor luminescence properties that these complexes showed in solution. In the $CHCl_3$ solutions spectra, **1-Sm, 2-Eu** and **3-Tb** show similar profile with a broad band showing to peak maxima. This is very similar to the absorption spectra obtained for those compounds, meanwhile, compound **6-Yb** shows band with a solely peak appearing at longer wavelengths. This may indicate that while sensitization of compounds **1-Sm**, **2-Eu** and **3-Tb** take place through both ligands, Btfa and also 4,4'-dinonyl-2,2'-bipy (lower wavelength peak), sensitization of **6-Yb** takes place through only the Btfa ligand. Singlet state of the β-diketone is less energetic than the polypyridyl N,N-donor ligand as seen in the absorption measurements. Since the emitting level

of the Yb^{3+} ion is of lower energy, Btfa may play a more important role in **6-Yb** sensitization effect.

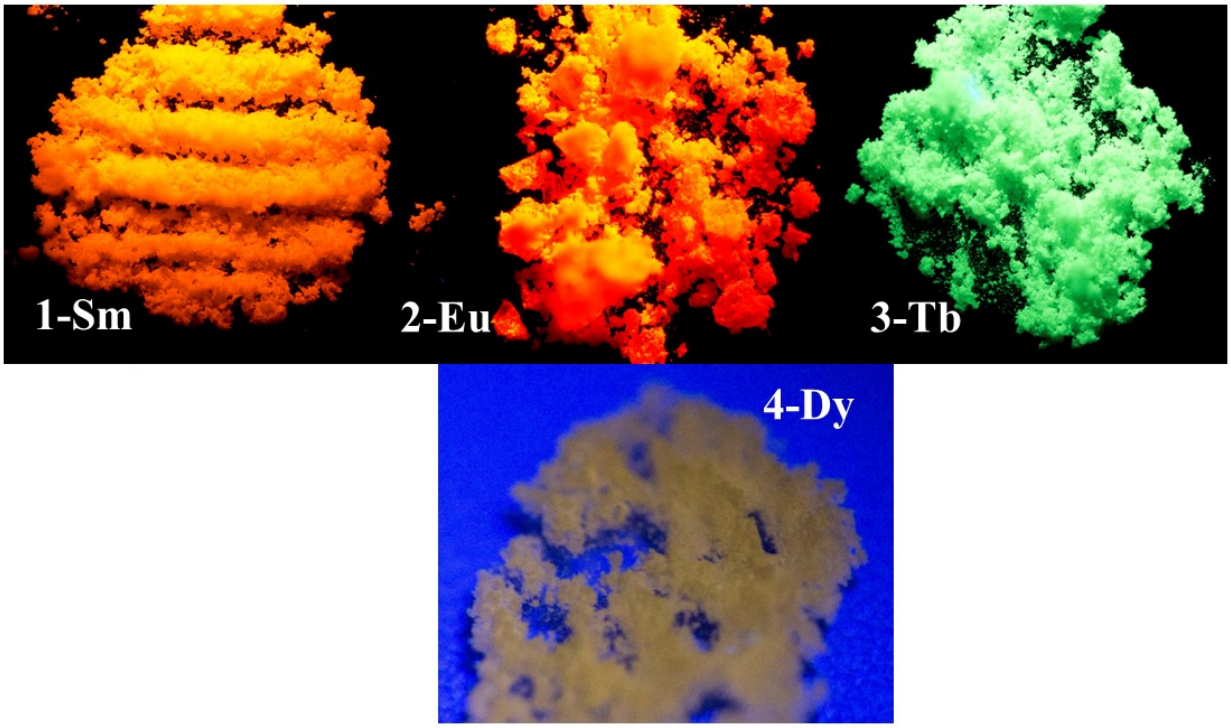

Fig. S8. a) Emission color observed by the naked eye of the polycrystalline samples of **1-Sm**, **2-Eu, 3-Tb** and **4-**Dy in $CHCl_3$ under the radiation of the laboratory UV lamp

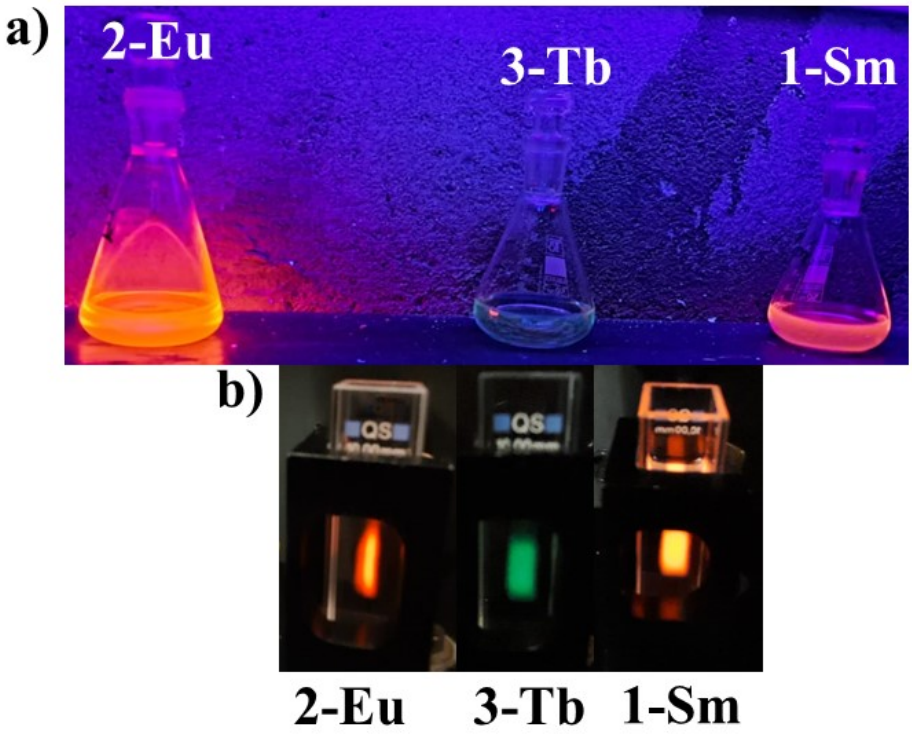

Fig. S9. a) Emission color observed by the naked eye of compounds **1-Sm**, **2-Eu** and **3-Tb** in $CHCl_3$ solution under the radiation of the laboratory UV lamp. b) and under 321 nm radiation.

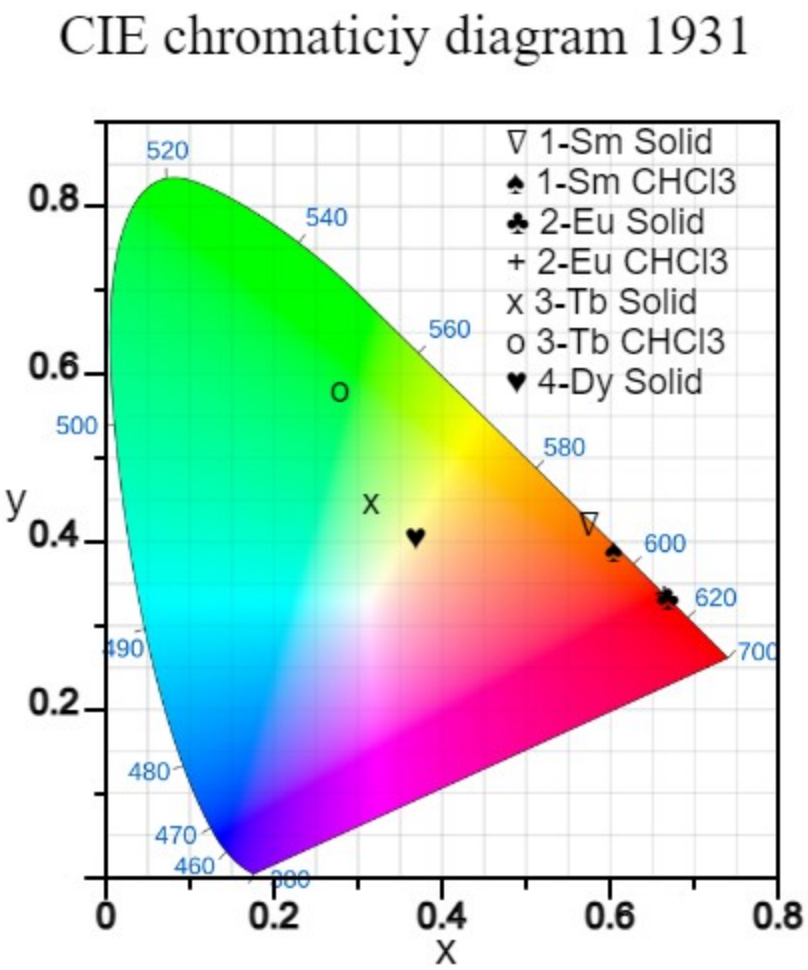

Figure S10. CIE chromaticity diagram 1931 colour coordinates, calculated for all emission spectra recorded in solid and solution state.

Table S3 a), b), c), d) and f). Wavelength assignation compilation to the emission transitions found in the emission spectra of the presented lanthanide coordination compounds.

1-Sm		
	Polycrystalline	**$1\cdot10^{-6}$M $CHCl_3$ solution**
$^4G_{5/2}\rightarrow{}^6H_{5/2}$	566 nm	564 nm
$^4G_{5/2}\rightarrow{}^6H_{7/2}$	609 nm	609 nm
$^4G_{5/2}\rightarrow{}^6H_{9/2}$	651 nm	647 nm

2-Eu		
	Polycrystalline	**$1\cdot10^{-6}$M $CHCl_3$ solution**
$^5D_0\rightarrow{}^7F_0$	581 nm	579 nm
$^5D_0\rightarrow{}^7F_1$	592 nm	591 nm
$^5D_0\rightarrow{}^7F_2$	614 nm	611 nm
$^5D_0\rightarrow{}^7F_3$	653 nm	651 nm
$^5D_0\rightarrow{}^7F_4$	707 nm	703 nm
$^4G_{5/2}\rightarrow{}^6H_{11/2}$	702 nm	709 nm

3-Tb		
	Polycrystalline	**$1\cdot10^{-6}$M $CHCl_3$ solution**
$^5D_4\rightarrow{}^7F_6$	492 nm	489 nm
$^5D_4\rightarrow{}^7F_5$	546 nm	545 nm
$^5D_4\rightarrow{}^7F_4$	583 nm	582 nm
$^5D_4\rightarrow{}^7F_3$	619 nm	618 nm
$^5D_4\rightarrow{}^7F_{2\text{-}1}$	658 and 681 nm	658 and 681 nm

4-Dy		
	Polycrystalline	**$1\cdot10^{-6}$M $CHCl_3$ solution**
$^7F_{9/2}\rightarrow{}^6H_{15/2}$	481 nm	-
$^7F_{9/2}\rightarrow{}^6H_{13/2}$	577 nm	-
$^7F_{9/2}\rightarrow{}^6H_{11/2}$	664 nm	-

5-Yb		
	Polycrystalline	**$1\cdot10^{-6}$M $CHCl_3$ solution**
$^7F_{5/2}\rightarrow{}^2F_{7/2}$	998 nm	999 nm

6-Er		
	Polycrystalline	**$1\cdot10^{-6}$M $CHCl_3$ solution**
$^4I_{13/2}\rightarrow{}^4I_{15/2}$	1524 nm	-

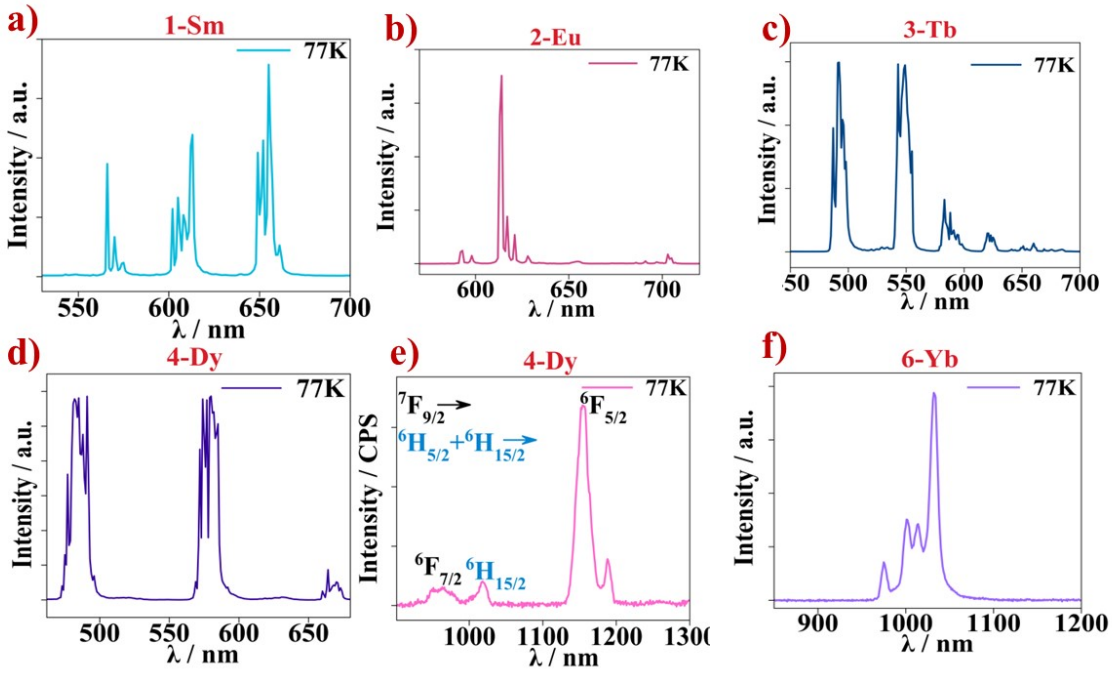

Fig. S11. Emission spectra measured at 77 K of the presented compounds **1-Sm** to **6-Yb** in the Visible a), b), c), d) and in the nIR range e) and f).

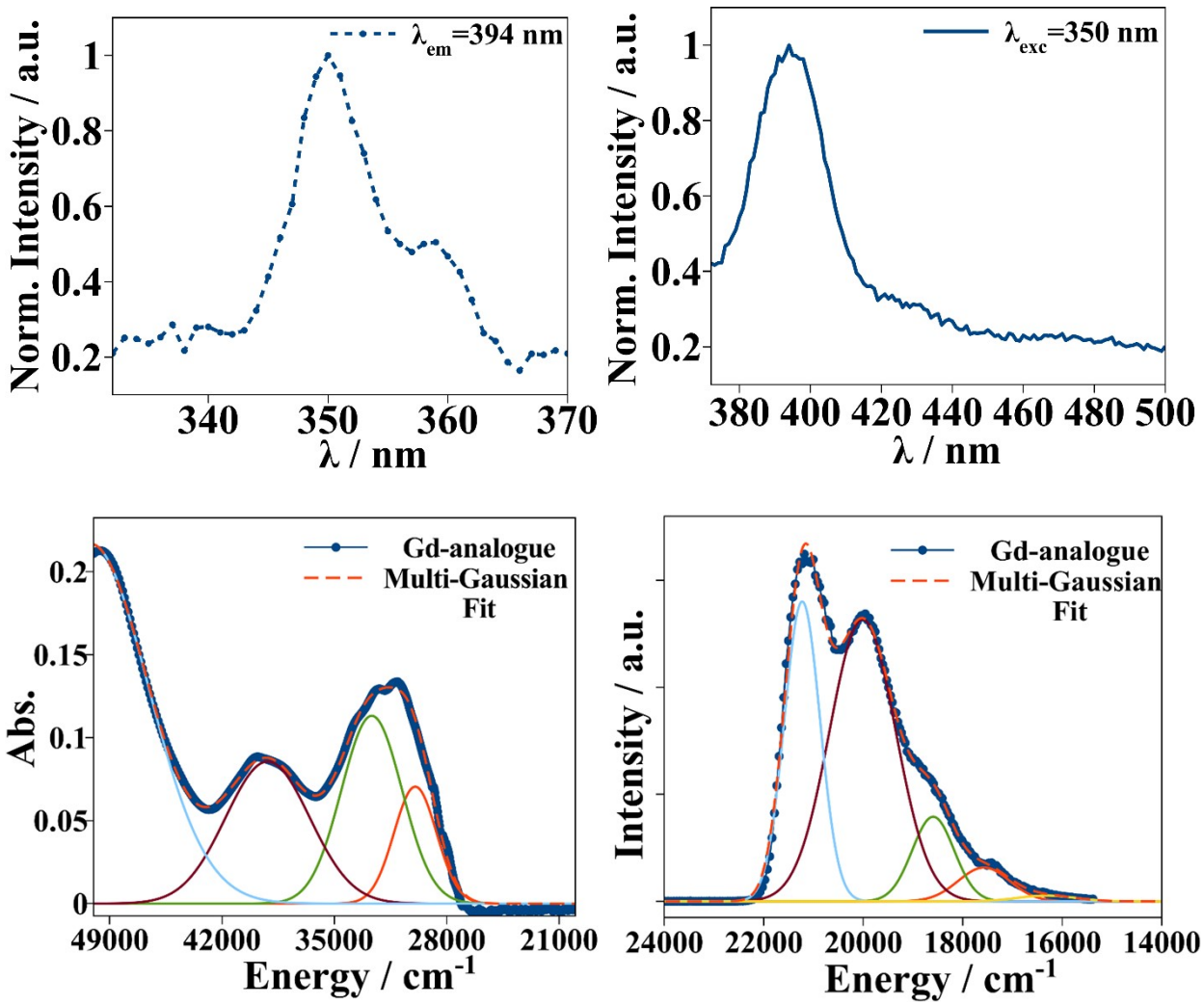

Figure S12 *Top left*, excitation spectrum of 1mM $CHCl_3$ solution of [Gd(Btfa)$_3$(4,4'-dinonyl-2,2'-bipy)] monitored at a λ_{em} of 394 nm. *Top right*, emission spectrum of 1mM $CHCl_3$ solution of [Gd(Btfa)$_3$(4,4'-dinonyl-2,2'-bipy)] monitored at a λ_{exc} of 350 nm. Excitation and emission bands found in spectra of [Gd(Btfa)$_3$(4,4'-dinonyl-2,2'-bipy)] are assigned to excitation and emission transitions from the ligand molecules. *Bottom left*, UV-Vis absorbance spectrum of compound [Gd(Btfa)$_3$(4,4'-dinonyl-2,2'-bipy)] measured on a 1mM $CHCl_3$ solution. Singlet state (S_1) is extracted from the edge of the Gaussian function form the multi-gaussian fit of the absorbance spectrum. *Bottom*, phosphorescence spectrum of 1mM $CHCl_3$ solution containing [Gd(Btfa)$_3$(4,4'-dinonyl-2,2'-bipy)] (λ_{exc}=336 nm). The band, corresponding to the ligands phosphorescence, was fitted with a multi-gaussian fit. Lowest triplet state (T_1) is obtained from the barycentre of the gaussian function found in the highest energy range.

1.3. Photoluminescence quantum yield (ϕ_{Ln}^{L}) and luminescence decay time (τ_{obs}):

The amount of energy absorbed by the chromophore ligands that is transferred to the excited state of the lanthanide ion is known as the sensitization efficiency (η_{sens}), and it plays a significant role in the overall quantum yield, which is defined as: $\phi_{Ln}^{L} = \eta_{sens} \cdot \phi_{Ln}^{Ln}$

The other factor that determines the ϕ_{Ln}^{L} value is the intrinsic quantum yield (ϕ_{Ln}^{Ln}) that alludes to the quantum yield once the emitting level of the lanthanide ion has been populated. The intrinsic quantum yield is related to the ratio between the measured time decay and the radiative lifetime τ_{rad} as shown in Eq. S1

$$\phi_{Ln}^{Ln} = \frac{k_r}{k_r + k_{nr}} = \frac{\tau_{obs}}{\tau_{rad}} \qquad \text{Eq. S1}$$

The radiative lifetime (τ_{rad}) is the luminescence lifetime in absence of non-radiative deactivations. Because of the pure magnetic dipole character that europium(III)'s $^5D_0 \rightarrow {}^7F_1$ transition, τ_{rad} from the $^5D_0$ emissive level can be calculated from the corrected emission spectrum and a simplified equation presented in Eq. S2 [1]:

$$\frac{1}{t_{rad}} = A_{MD,0} \times n^3 \left(\frac{I_{TOT}}{I_{MD}}\right) \qquad \text{Eq. S2}$$

$A_{MD,0}$ is a constant (14.65 cm^{-1}), n is the refractive index (1.517 for microcrystalline sample and 1.446 for chloroform solution, 20ºC) and $\frac{I_{TOT}}{I_{MD}}$ is the ratio between the total integrated area measured from the corrected Eu(III) emission spectrum (I_{TOT}) to the integrated area of the pure magnetic dipole transition $^5D_0 \rightarrow {}^7F_1$ (I_{MD}).

1.4 Organic light-emitting diodes

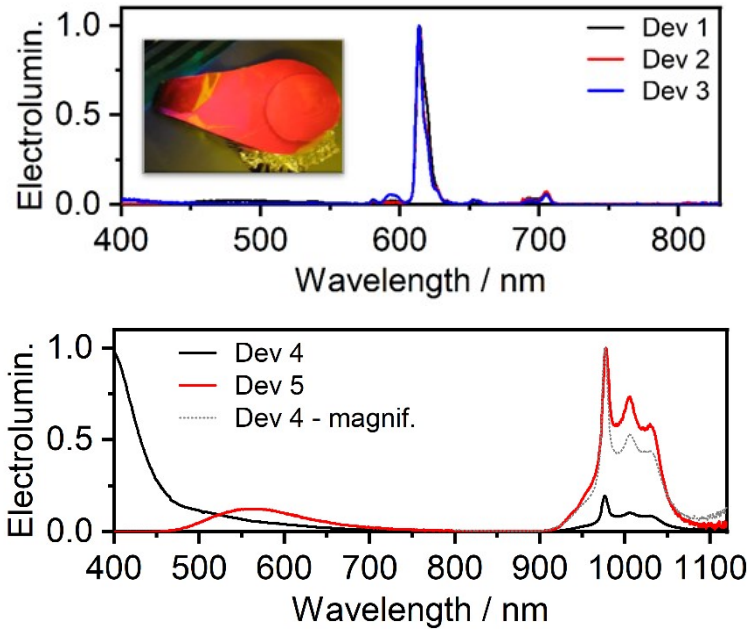

Fig. S13. Electroluminescence spectra of devices **1-5** from compounds **1-Eu** (Top) and **6-Yb** (Bottom). Inset top, photoluminescence from a film of **1-Eu** thermally deposited on aluminum foil (λ_{exc}=365 nm).

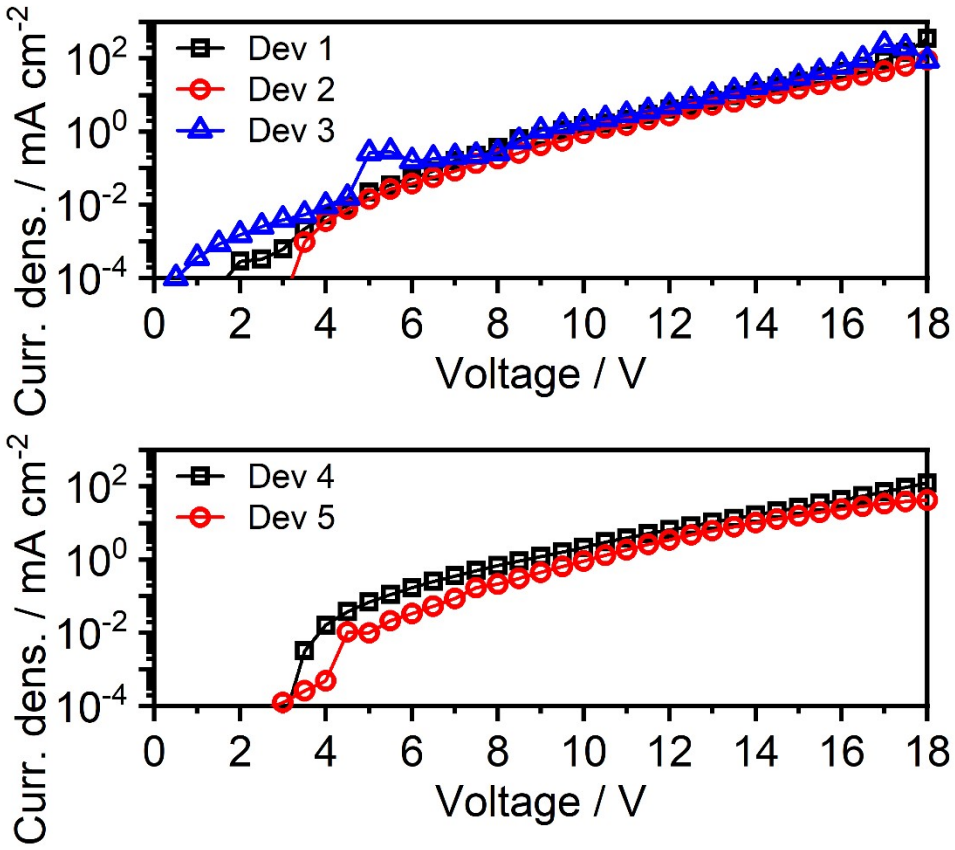

Fig. S14. Current Density vs. Voltage bias for devices **1-5**.

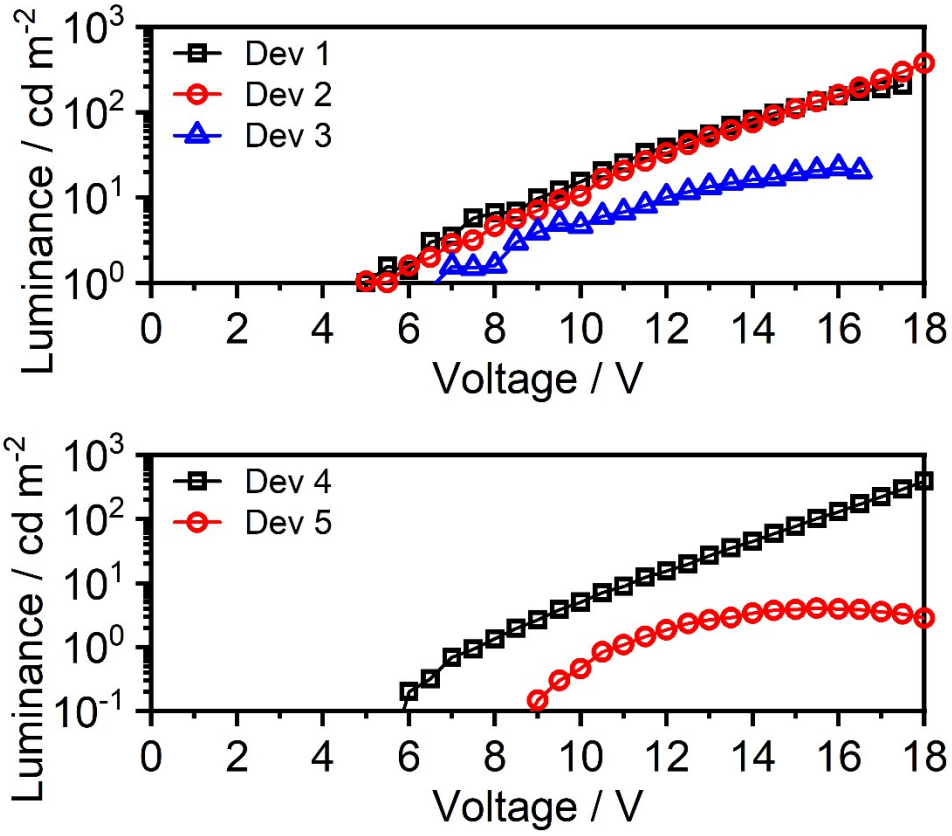

Fig. S15. Luminance vs. Voltage bias for devices **1-5.**

1.2 Magnetic measurements:

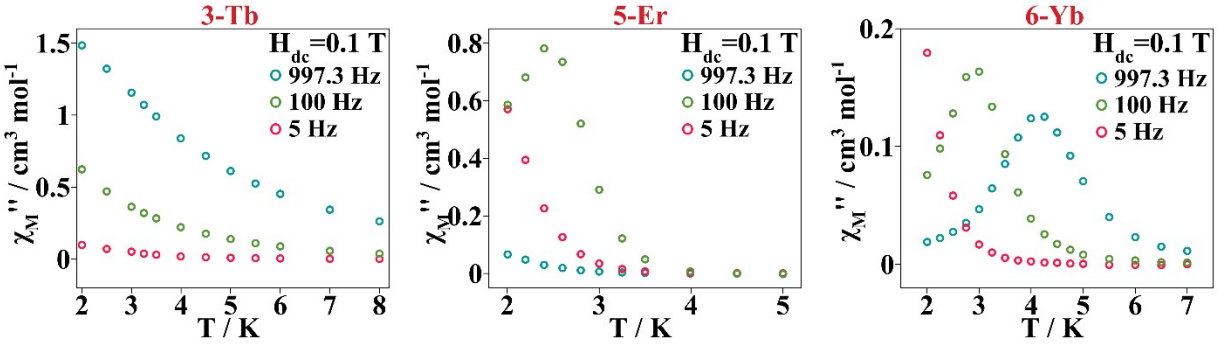

Fig. S16. χ_M'' component in front of the temperature measured at three frequencies of the $4 \cdot 10^{-4}$ T oscillating magnetic field and an external magnetic dc field of 0.1T for compounds **3-Tb**, **5-Er** and **6-Yb**. The χ_M'' shows dependence with temperature and frequency for the three compounds.

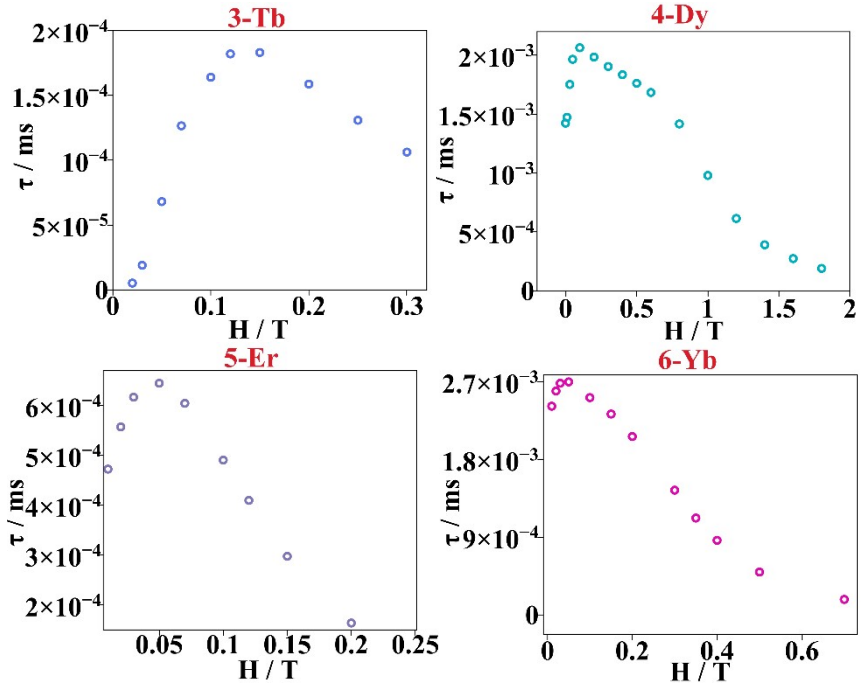

Fig. S17 Relaxation times (1/2πν) in front of different static magnetic fields measured at a constant temperature of 2K for **3-Tb** and **5-Er**, 11 K for **4-Dy** and 2.75 K for **6-Yb** under an ac magnetic field of 4·10-4 T oscillating between 1 to 1488 Hz.

$$\chi_{AC}(\omega) = \chi_S + \frac{\chi_T - \chi_S}{1 + (i\omega\tau)^{(1-\alpha)}}$$

Eq. S3. Generalized Debye model that describes a system with a distribution of the magnetization relaxation time. Where χ_S and χ_T are the adiabatic and thermal susceptibilities, τ is the relaxation of the magnetization time and ω is the angular frequency of the ac field ($\omega = 1/2\pi f$). χ_T is the susceptibility in the limit of the lowest field frequencies where the thermal equilibrium of the system is observed. χ_S (lower than the χ_T) is observed when the oscillations of the ac field are fast compared to the time constant, τ, and the magnetic system remains isolated from its environment. The α parameter quantifies the width of the τ distribution and it ranges from 0 to 1. The wider the time distribution, α acquires a larger value.

T/K	χ_S/ cm^{3}mol^{-1}	χ_T/ cm^{3}mol^{-1}	τ /s	α
2.5	0.0899994	5.6966808	0.0239962	0.243565
3	0.0808478	4.784409	0.0237388	0.2470289
3.5	0.0688829	4.1410772	0.0235062	0.2499711
4	0.0634415	3.6401817	0.0229922	0.2475158
4.5	0.0593894	3.2141338	0.0219038	0.2405165
5	0.0583447	2.8899059	0.0205298	0.2277201
5.5	0.0583902	2.6156656	0.0185999	0.2092533
6	0.0582438	2.3773577	0.0162939	0.1864077
6.5	0.0578338	2.1799846	0.0138781	0.1604597
7	0.0556806	2.0071623	0.0115571	0.1371048
7.5	0.0523509	1.8620869	0.0094869	0.1166131
8	0.0491802	1.7375743	0.0076983	0.0985174
8.5	0.045822	1.6297371	0.006171	0.0837034
9	0.0424934	1.5352533	0.0048814	0.0714849
9.5	0.0392212	1.4517602	0.00379	0.0617365
10	0.0367583	1.3774303	0.0028693	0.0540821
10.4	0.0345922	1.3102725	0.0020924	0.0484347
10.9	0.0326136	1.2451281	0.001419	0.0447284
11.3	0.0323025	1.1870709	9.22E-04	0.0418099
12	0.0365019	1.1081857	4.43E-04	0.0383483
12.5	0.0444623	1.062124	2.70E-04	0.0343113
13	0.0562949	1.0197036	1.64E-04	0.029758
13.5	0.0735509	0.9807693	1.00E-04	0.0279038

Table S4. Values of the parameters obtained from the fit using the Generalized Debye model function for compound **4-Dy** from the ac magnetic measurements at different temperatures at a 0 external magnetic field.

T/K	χ_S/ cm^{3}mol^{-1}	χ_T/ cm^{3}mol^{-1}	τ /s	α
5	0.025755273	2.894972045	0.434302279	0.049943799
5.5	0.025183443	2.523949348	0.21968462	0.035531107
6	0.02440133	2.295606999	0.125936886	0.028754592
6.5	0.024135394	2.112338	0.076794128	0.023851869
7	0.022032696	1.959084046	0.048900038	0.021727093
7.5	0.02175058	1.828746726	0.032463862	0.019858225
8	0.021403515	1.715719499	0.022162438	0.018695676
8.5	0.019455247	1.616759621	0.015377077	0.019421731
9	0.01933141	1.528721829	0.010758944	0.020262677
9.5	0.01968522	1.449606371	0.007499486	0.021812518
10	0.020250793	1.378695329	0.00513716	0.025037769
10.4	0.020763265	1.313902582	0.003395967	0.030618168
10.9	0.021949555	1.250758666	0.002072573	0.036163797
11.3	0.023388448	1.195209002	0.001219484	0.04334925
12	0.028489691	1.114714156	5.07E-04	0.047359711
12.5	0.029950994	1.068339329	2.84E-04	0.049900342
13	0.029937286	1.02565476	1.61E-04	0.051643359
13.5	0.029842153	0.986216068	9.20E-05	0.053771433

Table S5. Values of the parameters obtained from the fit using the Generalized Debye model function for compound **4-Dy** from the ac magnetic measurements at different temperatures at direct current external magnetic field of 0.1 T.

T/K	χ_S/cm^{3}mol^{-1}	χ_T/cm^{3}mol^{-1}	τ /s	α
1.8	0.12152	5.17077	0.00018	0.27268
1.9	0.06319	4.98984	0.00016	0.27918
2	0.00583	4.77019	0.00015	0.28254
2.1	0.0012	4.5873	0.00014	0.27814
2.3	0.01233	4.33987	0.00013	0.26656
2.5	0.0372	4.09429	0.00012	0.2546
2.7	0.05996	3.86918	0.00011	0.24367
2.9	0.07411	3.66271	0.00011	0.23508
3.1	0.07206	3.47414	9.9E-05	0.23014
3.4	0.0723	3.22011	8.9E-05	0.22363
3.7	0.07027	2.99735	8.1E-05	0.22001

Table S6. Values of the parameters obtained from the fit using the Generalized Debye model function for compound **3-Tb** from the ac magnetic measurements at different temperatures at direct current external magnetic field of 0.1 T.

T/K	χ_S/cm^{3}mol^{-1}	χ_T/cm^{3}mol^{-1}	τ /s	α
1.82727	0.40426	2.67227	0.00092	0.08266
1.88597	0.39162	2.56991	0.00077	0.08058
1.99649	0.3812	2.44627	0.0006	0.07118
2.09694	0.37131	2.33912	0.00047	0.06235
2.20135	0.36627	2.2753	0.0004	0.05557
2.3008	0.35014	2.17278	0.00029	0.04853
2.4019	0.33859	2.09102	0.00022	0.04082
2.50126	0.32079	2.01706	0.00016	0.0368
2.60047	0.29962	1.94926	0.00012	0.03266
2.70054	0.27142	1.88614	8.7E-05	0.02975

Table S7. Values of the parameters obtained from the fit using the Generalized Debye model function for compound **5-Er** from the ac magnetic measurements at different temperatures at direct current external magnetic field of 0.07 T.

T/K	χ_S/cm^{3}mol^{-1}	χ_T/cm^{3}mol^{-1}	τ /s	α
2.1	0.03552	0.55693	0.01185	0.15778
2.3	0.03235	0.50111	0.00737	0.123
2.5	0.03041	0.45015	0.00445	0.08537
2.7	0.02808	0.41547	0.00282	0.06772
2.9	0.0245	0.38542	0.0018	0.05532
3.1	0.02194	0.36068	0.00119	0.04713
3.4	0.01799	0.32976	6.58E-04	0.03771
3.7	0.01439	0.30297	3.81E-04	0.03035
4	0.01228	0.28052	2.30E-04	0.02112
4.3	0.00555	0.26081	1.43E-04	0.02068

Table S8. Values of the parameters obtained from the fit using the Generalized Debye model function for compound **6-Yb** from the ac magnetic measurements at different temperatures at direct current external magnetic field of 0.1 T.

Table S9. Compilation of the fitted parameters from the relaxation of the magnetization mechanisms of compounds **3-Tb**, **4-Dy**, **5-Er** and **6-Yb**.

	H_{dc} (T)	Orbach		QTM	Raman		Direct
		ΔE (cm^{-1})	τ_0 (s)	τ_{QTM} (s)	C s^{-1}K^{-n}	n	A s^{-1}K^{-1}
3-Tb	0.1				0.93	5.2	3275.14
4-Dy	0	103.7	$2.53\cdot10^{-9}$	0.03	$8.18\cdot10^{-4}$	5.5	
	0.1	140.5	$3.6\cdot10^{-11}$		$1.10\cdot10^{-4}$	6.2	
5-Er	0.05	24.64	$8.75\cdot10^{-8}$		96.1	4.05	
6-Yb	0.05				0.51	6.5	8.58

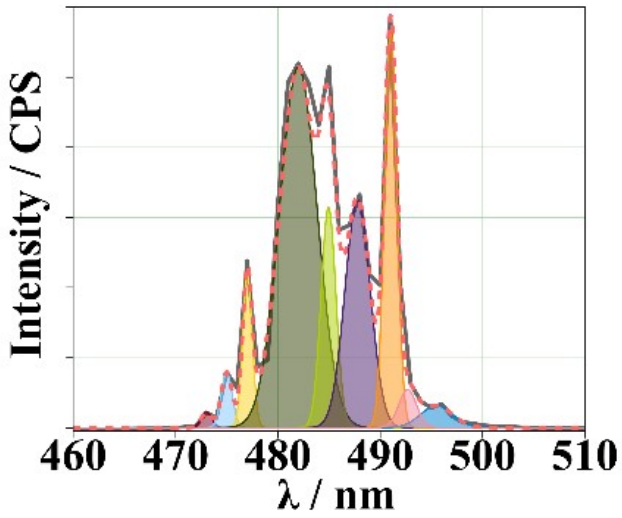

Fig. S18 $^{7}F_{9/2}\rightarrow{}^{6}H_{15/2}$ emission band measured at 77K of **4-Dy**. Grey continuous line is the experimental emission band. Scattered red line is the total multi-Gaussian fit.

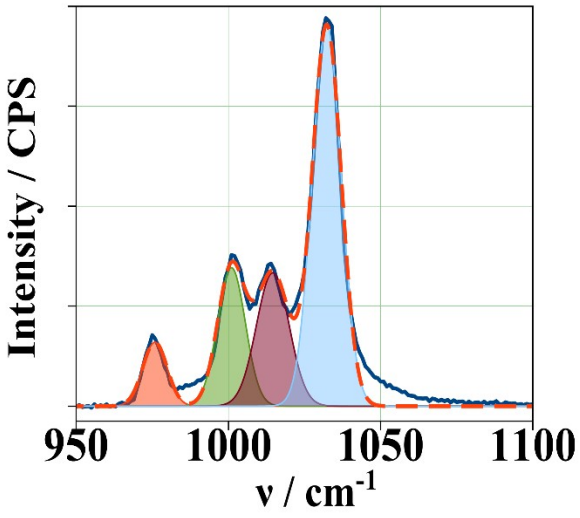

Fig. S19 $^{2}F_{5/2}\rightarrow{}^{2}F_{7/2}$ emission band measured at 77K of **6-Yb**. Blue continuous line is the experimental emission band. Scattered red line is the total multi-Gaussian fit.

1.5. References:

[1] M. H. V. Werts, R. T. F. Jukes, J. W. Verhoeven, *Phys. Chem. Chem. Phys.*, **2002**, 4, 1542.